

Accelerated Publications

A Noncanonical Tertiary Conformation of a Human Mitochondrial Transfer RNA[†]

Maureen A. Leehey, Christine A. Squassoni, Marisa W. Friederich, Janine B. Mills, and Paul J. Hagerman*

Departments of Neurology and Biochemistry, Biophysics, and Genetics, University of Colorado Health Sciences Center, Denver, Colorado 80262

Received September 28, 1995; Revised Manuscript Received October 31, 1995[®]

ABSTRACT: Transfer RNAs possess highly conserved secondary structures, and crystallographic studies suggest a common, L-shaped tertiary conformation in which the anticodon and acceptor stems are disposed at approximately right angles to one another. However, many animal mitochondrial tRNAs possess unusual secondary structures, and little is known regarding their tertiary conformations, in particular, the relative orientations of their acceptor and anticodon stems. To address this issue, we have constructed heteroduplex RNA molecules corresponding to human mitochondrial and cytoplasmic lysyl tRNAs in which the acceptor and anticodon stems of each tRNA have been extended by approximately 70 base pairs. The rotational decay times of the two "extended" tRNA^{Lys} species were compared to the decay times of a linear RNA control and to an extended yeast cytoplasmic tRNA^{Phe} species whose interstem angle had been reported previously. Whereas the apparent interstem angle of the human cytoplasmic tRNA^{Lys} species is essentially identical to that of the yeast tRNA^{Phe} heteroduplex, with both conforming to the canonical L-shape, the angle for the mitochondrial tRNA^{Lys} construct is much larger (~140°). Thus, the universal L-shape may not be applicable to noncanonical mitochondrial tRNAs, a finding of significance for both tRNA evolution and mitochondrial disease.

Transfer RNAs of widely divergent phylogenetic origins have highly conserved cloverleaf secondary structures that can be further folded into a canonical L-shaped tertiary conformation (Sussman et al., 1978; Hingerty et al., 1978; Westhof et al., 1985; Woo et al., 1980; Schevitz et al., 1979; Friederich, et al., 1995). However, many animal mitochondrial tRNAs are unusual in that they lack the invariant nucleotides in the dihydrouridine and T ψ C loops thought to be necessary for tertiary folding. Absent a crystal structure, studies on mitochondrial tRNAs have employed enzymatic and chemical probing, phylogenetic comparison, and com-

puter modeling to predict tertiary structure. These approaches have led to the notion that noncanonical mitochondrial tRNAs fold into the canonical L-shaped conformation (de Bruijn & Klug, 1983; Ueda et al., 1985; Yokogawa et al., 1989, 1991; Wakita et al., 1994; Watanabe et al., 1994). However, on the basis of computer modeling, it has been proposed that some mitochondrial tRNAs may have a broader angle between the arms comprising the "L" in order to maintain a constant distance between the anticodon and acceptor ends (Steinberg et al., 1994; Steinberg & Cedergren, 1994).

In an effort to determine whether unusual mitochondrial tRNAs possess a tertiary conformation similar to the L form of canonical tRNAs, we have utilized the method of transient electric birefringence (TEB). This method allows us to measure directly the angle subtending the anticodon and acceptor stems of human mitochondrial tRNA^{Lys}, which

[†] Supported by Grants GM35305 (to P.J.H.) and AG00621 (M.A.L.) from the National Institutes of Health and by facilities support from the Lucille P. Markey Charitable Trust.

* Correspondence to this author at the Department of Biochemistry, Biophysics, and Genetics, University of Colorado Health Sciences Center, 4200 E. 9th Ave., Box B121, Denver, CO 80262.

[®] Abstract published in *Advance ACS Abstracts*, December 1, 1995.

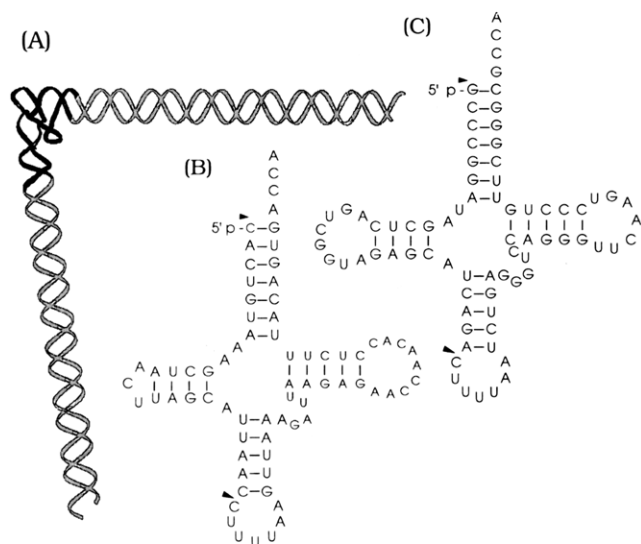


FIGURE 1: (A) Schematic representation of the heteroduplex tRNA constructs used in the current study. (B) Secondary structure of human mitochondrial tRNA^{Lys} (Anderson et al., 1981). (C) Secondary structure of human cytoplasmic tRNA^{Lys}(AAA) (Roy et al., 1982). The arrowheads indicate the points of extension of the acceptor and anticodon helices.

departs significantly from the canonical tRNA secondary structure (Figure 1). The TEB method is particularly well suited for quantifying the angles formed between helix stems that flank centrally located bulges or other nonhelix elements (Friederich et al., 1995; Shen & Hagerman, 1994; Amiri & Hagerman, 1994; Zacharias & Hagerman, 1995a,b) and has been used to determine the interstem angle for yeast tRNA^{Phe} transcripts (Friederich et al., 1995). In a typical TEB experiment, the element of interest is placed in the center of an RNA helix such that the nonhelix element is flanked by helices of 50–100 bp. By virtue of the more rapid rotational diffusion experienced by bent or flexible heteroduplex molecules relative to fully duplex controls, the helix extensions “report” the apparent interhelix angles of the element of interest. This approach is exactly analogous to the earlier investigation of DNA four-way junctions using TEB (Cooper & Hagerman, 1989).

In the current work, tRNA derivatives in which the anticodon and acceptor stems have been extended by approximately 70 bp were produced as heteroduplex molecules from pairs of *in vitro* (T7 polymerase) RNA transcripts (Friederich et al., 1995; Figures 1 and 2). Specifically, the extended (E) heteroduplexes corresponding to human mitochondrial tRNA^{Lys} (E[hmtRNA^{Lys}]), human cytoplasmic tRNA^{Lys}(AAA) (E[hctRNA^{Lys}(AAA)]), and yeast cytoplasmic tRNA^{Phe} (E[yctRNA^{Phe}]) were assembled, and their gel electrophoretic and TEB behaviors were compared to those of a linear duplex (174 bp) RNA molecule in a fashion that is strictly analogous to the previously published investigation of yeast tRNA^{Phe} (Friederich et al., 1995). The mitochondrial species exhibits gel mobility and TEB properties that are indicative of a much broader interstem angle than either of the cytoplasmic species.

MATERIALS AND METHODS

Preparation of RNA Expression Plasmids. The DNA oligomers used for the construction of the expression plasmids for the extended (human) tRNA heteroduplexes are

listed in Table 1. Each insert is located at the center of a 136-nucleotide transcription template in either pGJ122A and pGJ122B RNA (T7-based) expression plasmids (Friederich et al., 1995); the two plasmids differ only in the orientation of the 136-nt template. Plasmids used for the production of the yeast tRNA transcripts and the linear (174 bp) control are as described elsewhere (Friederich et al., 1995). All other procedures for the construction, purification, and characterization of the resulting plasmids are as described (Friederich et al., 1995).

Preparation of the Duplex and Heteroduplex RNA Molecules. The basic outline for the formation of the heteroduplex tRNA molecules is presented in Figure 2. Transcription reactions, transcript purification, and annealing reactions were carried out essentially as described previously (Amiri & Hagerman, 1994; Zacharias & Hagerman, 1995a; Friederich et al., 1995). Heteroduplex and duplex RNA molecules were analyzed for degradation on gels, both prior to and following the TEB experiments. The TEB measurements resulted in no detectable degradation of any of the RNA species.

Gel Electrophoresis. Polyacrylamide gels were prepared from 10% acrylamide [19:1 monomer:*N,N'*-methylenebis(acrylamide) ratio] and were run at approximately 25 °C with buffer recirculation. For the gels lacking Mg²⁺ ions, the running buffer was 10 mM sodium phosphate (pH 7.2) and 0.125 mM NaEDTA; for the gels containing 1 mM MgCl₂, the running buffer was 10 mM sodium phosphate without added EDTA. Relative electrophoretic mobility refers to the ratio of the mobility of a heteroduplex RNA to the mobility of the linear control.

Transient Electric Birefringence (TEB) Measurements. TEB measurements were performed and analyzed essentially as described previously (Zacharias & Hagerman, 1995a; Friederich et al., 1995). The pulse width was 1 μs, amplitude 2.0 kV (field strength = 10 kV), and repetition frequency 1 Hz. Each measurement represents the average of 128 pulses. Measurements were performed at 3.5 °C. The averaged birefringence decay curves were analyzed as double-exponential functions using the Levenberg–Marquardt method (Press et al., 1992).

Determination of the Acceptor–Anticodon Interstem Angles from the Birefringence Decay Data. The apparent interstem angles were determined exactly as described previously (Friederich et al., 1995), using the program DIFFROT to determine the relationship between the observed τ -ratios ($\tau_{\text{E[RNA]}}/\tau_{\text{duplex}}$) and the interstem angles [see Figure 3 of Friederich et al. (1995)]. A suitable interpolation formula for the current study is

$$\theta = 180^\circ - \{a \cos^{-1} R + 0.005[\sin^{-1}(1 - R)]^b\}$$

where R is the experimental τ -ratio, $a = 1.458$, $b = 2.2727$, and θ is the apparent interstem angle in degrees.

RESULTS AND DISCUSSION

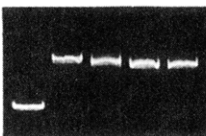
A gel electrophoretic analysis (Figure 3) of the E[tRNA] constructs reveals that the two cytoplasmic forms, E[hctRNA^{Lys}(AAA)] and E[yctRNA^{Phe}], display relative mobilities that are nearly identical to one another, in both the presence and absence of Mg²⁺ ions. These observations are entirely consistent with the notion that all tRNAs possess the canonical L-shaped global conformation. However, the

species ^a	insert ^b	plasmid/orientation ^c
hmtRNA/5' half	5'-AGCTGGT▼CACTGTAAAGCTAACTTAGCATTAAC▼GCT CCA GTGACATTTTCGATTGAATCGTAATTG CGATCGA-5'	pGJ122A
hmtRNA/3' half	5'-AGCTAGC▼GTAAAGATTAAGAGAACCAACACCTCTTTACAGTG▼ACC TCG CAATTTCTAATTCTCTTGGTTGTGGAGAAATGTCAC TGGTCGA-5'	pGJ122B
hctRNA/5' half	5'-AGCTGGT▼GCCCGGATAGCTCAGTCGGTAGAGCATCAGA▼GCT CCA CGGGCCTATCGAGTCAGCCATCTCGTAGTCT CGATCGA-5'	pGJ122A
hctRNA/3' half	5'-AGCTAGC▼TCTGAGGGTCCAGGGTTCAAGTCCCTGTTCCGGGC▼ACC TCG AGACTCCCAGGTCCCAAGTTCAGGGACAAGCCCG TGGTCGA-5'	pGJ122B

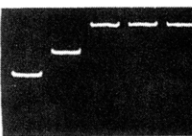
The diagram illustrates the construction and RNA processing of the pGJ122(A,B) plasmid. The plasmid map at the top shows a T7 promoter, an insert site (H), and a SalI (S) site. Transcription starts at the T7 promoter. The resulting RNA transcripts are shown annealing to form a dimeric structure. The 73 bp regions are highlighted with arrows.

The principal (qualitative) conclusions of the gel experiments have been confirmed through a series of quantitative TEB measurements, in which the birefringence decay times of the E[tRNA] species were compared to the decay time of the linear control (Figure 4). The results of these measure-

(A)



(B)



(C)

MgCl ₂	human E[trnALys] mitochondrial	human E[trnALys] cytoplasmic	yeast E[trnAPhe] cytoplasmic
0	0.53	0.58	0.61
1.0 mM	0.67	0.25	0.25

In the absence of magnesium and spermine, the cytoplasmic constructs are more open, with the E[yctRNA^{Phe}] species possessing an angle of $151 \pm 0.6^\circ$, while the E[hctRNA^{Lys(AAA)}] becomes essentially collinear; these changes probably reflect general unfolding of the tRNA core. However, E[hmtRNA^{Lys}] becomes slightly *less* open, with an interstem angle of $131 \pm 0.3^\circ$. All of these observations are consistent with the gel mobility results. Thus, the addition of magnesium induces the cytoplasmic species to become more folded, while the mitochondrial species becomes more linear. The two cytoplasmic species have

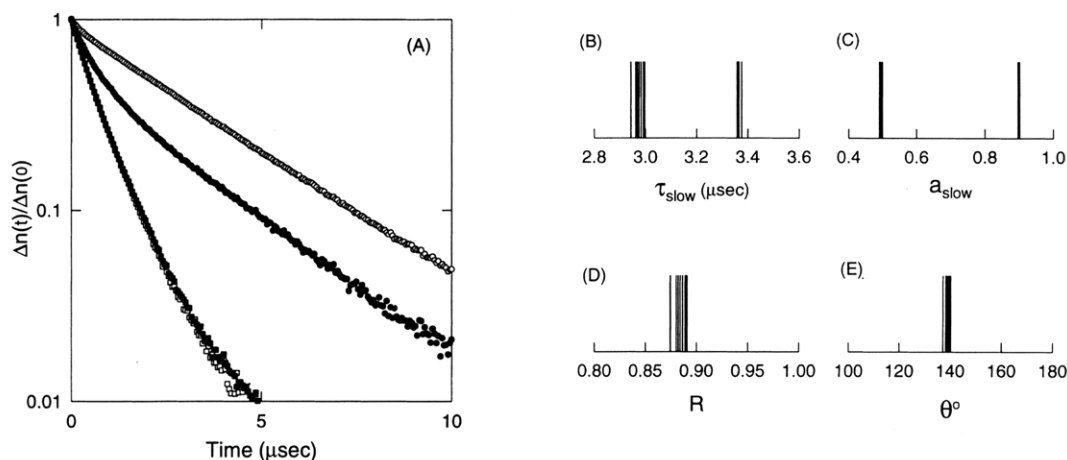


FIGURE 4: (A) Representative semilogarithmic plots of transient electric birefringence (TEB) decay curves for the E[tRNA] species: (filled circle) E[hmtRNA^{Lys}]; (filled square) E[hctRNA^{Lys(AAA)}]; (open square) E[yctRNA^{Phe}]; (open circle) 174 bp linear RNA control. $\Delta n(t)$ is the sample birefringence at time t , and $\Delta n(0)$ is the birefringence at $t = 0$. (B) Distribution of terminal (slow) decay times (τ_{slow}) for E[hmtRNA^{Lys}] ($2.98 \pm 0.018 \mu\text{s}$) and the linear control ($3.36 \pm 0.007 \mu\text{s}$). (C) Fractional amplitudes (a_{slow}) associated with the terminal decay components for E[hmtRNA^{Lys}] (0.49 ± 0.003) and the linear control (0.90 ± 0.002). (D) Ratios obtained from (B) as $R = \tau_{\text{slow}}(\text{E[hmtRNA}^{\text{Lys}}]) / \langle \tau_{\text{slow}}(\text{linear}) \rangle$. (E) Distribution of apparent angles (mean = 139.2°) from R and computed τ -ratio plots (Friederich et al., 1995; Zacharias & Hagerman, 1995a).

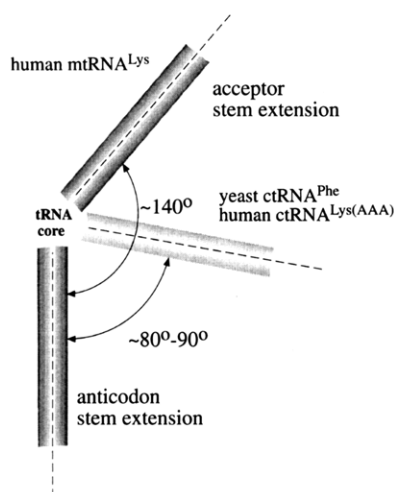


FIGURE 5: Summary of the results of TEB measurements for the human mitochondrial tRNA^{Lys} construct (E[hmtRNA^{Lys}]) and the yeast and human cytoplasmic constructs (E[yctRNA^{Phe}] and E[hctRNA^{Lys(AAA)}]). The constructs are designated by their core tRNA sequences.

nearly equal interstem angles for sufficiently high magnesium concentrations, both approximating the canonical L-shape. By contrast, the apparent interstem angle for the mitochondrial species ($\sim 140^\circ$) indicates a striking departure from the canonical form (Figure 5).

In considering this latter observation, two features of the current experiments should be noted. First, the tRNA cores have not been subjected to posttranscriptional modification. Even though the unmodified cytoplasmic species have interstem angles consistent with canonical tRNAs, the absence of specific, modified nucleotides could influence the results for the mitochondrial tRNA core. This issue is of particular importance for the mitochondrial species, which may be intrinsically less stable than its cytoplasmic counterpart (Kumazawa et al., 1989). However, the principal consequence of the absence of modified nucleotides is probably reduced thermal stability (Sampson & Uhlenbeck, 1988), not a substantial change in tertiary conformation. This contention is supported by the finding that the unmodified mitochondrial bovine tRNA^{Ser(AGY)} transcript and the native

tRNA^{Ser(AGY)} are aminoacylated at similar rates by the cognate synthetase (Ueda et al., 1992). Moreover, the angles presented in Figure 5 represent “limiting”, low-temperature conformations for the E[tRNA] species, since further additions of MgCl₂, or increases in temperature, have little effect on either the electrophoresis or TEB results.

Second, the current results do not rule out an intrinsically reduced structural rigidity of the mitochondrial tRNA core. To address this question, the E[tRNA] species were electrophoresed in varying polyacrylamide concentrations. The decrease in gel mobility with increasing polyacrylamide concentration is smaller for the mitochondrial species than for the two cytoplasmic species (data not shown) (Mills et al., 1994). In addition, the slow-phase amplitude of E[hmtRNA^{Lys}], $a_{\text{slow}} = 0.49$ (Figure 3C), is somewhat lower than the corresponding amplitudes ($a_{\text{slow}} \approx 0.5$ – 0.7) for RNA bulges possessing interhelix angles in the 40 – 50° range (Zacharias & Hagerman, 1995a). Both of these findings are consistent with the presence of some additional flexibility, which would not be surprising in view of the fact that some mitochondrial tRNAs lack the invariant nucleotides in the T ψ C and dihydrouridine loops that are thought to be important for stabilization of tertiary structure.

If the broad interstem angle of human mitochondrial tRNA^{Lys} is characteristic of all the tRNAs within animal mitochondria, it may signify that the mitochondrial machinery for protein synthesis is inherently different from the cytoplasmic machinery with respect to its utilization of tRNAs. This hypothesis is worth considering in light of the fact that 5S rRNA is absent from the ribosomes of multicellular animal mitochondria (Wolstenholme, 1992). It is also possible that some mitochondrial tRNAs have broader interstem angles to compensate for a smaller size. On the basis of computer modeling, Steinberg et al. (1994) proposed that mitochondrial tRNAs that completely lack a dihydrouridine stem may compensate for their smaller size by forming a more open “boomerang” tertiary conformation. Steinberg et al. (1994) further propose that there may be a universal constraint in the tertiary structure of all tRNAs, namely, that all tRNAs have the same distance between their anticodon and acceptor ends. Thus, some noncanonical

tRNAs may compensate for their smaller size by increasing their interstem angle to conserve that distance. Our observation of a more open interstem angle for human mitochondrial tRNA^{Lys} would appear to be generally supportive of the model of Steinberg et al. However, in apparent contrast to their model, human mitochondrial tRNA^{Lys} does possess a well-defined dihydrouridine stem and bridging nucleotides (Figure 1B).

In summary, the current study suggests that at least one mitochondrial tRNA from the human complement possesses a much larger interstem angle than do canonical tRNAs. The TEB method, which affords the advantage of directly measuring the interstem angle, can be used to further study these unusual tRNAs. In addition, the TEB method should be useful in studying the structural consequences of mitochondrial tRNA mutations such as the pathogenic point mutation in human mitochondrial tRNA^{Lys} that is associated with the syndrome of myoclonic epilepsy and ragged red fibers (MERRF) (Shoffner et al., 1990). This tRNA mutation represents one of more than two dozen human diseases thought to arise from point mutations in mitochondrial tRNAs.

ACKNOWLEDGMENT

The authors thank Elsi Vacano for carrying out the hydrodynamic computations using DIFFROT and Dr. Robert Cedergren for useful discussions and for providing manuscripts prior to publication.

REFERENCES

- Amiri, K. M. A., & Hagerman, P. J. (1994) *Biochemistry* 33, 13172–13177.
- Anderson, S., Bankier, A. T., Barrell, B. G., de Bruijn, M. H. L., Coulson, A. R., Drouin, J., Eperon, I. C., Nierlich, D. P., Roe, B. A., Sanger, F., Schreier, P. H., Smith, A. J. H., Staden, R., & Young, I. G. (1981) *Nature* 290, 455–465.
- Cooper, J. P., & Hagerman, P. J. (1989) *Proc. Natl. Acad. Sci. U.S.A.* 86, 7336–7340.
- de Bruijn, M. H. L., & Klug, A. (1983) *EMBO J.* 2, 1309–1321.
- Friederich, M. W., Gast, F.-U., Vacano, E., & Hagerman, P. J. (1995) *Proc. Natl. Acad. Sci. U.S.A.* 92, 4803–4807.
- Hingerty, B., Brown, R. S., & Jack, A. (1978) *J. Mol. Biol.* 124, 523–534.
- Kumazawa, Y., Yokogawa, T., Hasegawa, E., Miura, K., & Watanabe, K. (1989) *J. Biol. Chem.* 264, 13005–13011.
- Mills, J. B., Cooper, J. P., & Hagerman, P. J. (1994) *Biochemistry* 33, 1797–1803.
- Press, W. H., Vetterling, W. T., Teukolsky, S. A., & Flannery, B. P. (1992) *Numerical recipes in Fortran: The art of scientific computing*, pp 678–683, Cambridge University Press, Cambridge, U.K.
- Roy, K., Cooke, H., & Buckland, R. (1982) *Nucleic Acids Res.* 10, 7313–7322.
- Sampson, J. R., & Uhlenbeck, O. C., (1988) *Proc. Natl. Acad. Sci. U.S.A.* 85, 1033–1037.
- Schevitz, R. W., Podjarny, A. D., Krishnamachari, N., Hughes, J. J., & Sigler, P. B. (1979) *Nature* 278, 188–190.
- Shen, Z., & Hagerman, P. J. (1994) *J. Mol. Biol.* 241, 415–430.
- Shoffner, J. M., Lott, M. T., Lezza, A. M., Seibel, P., Ballinger, S. W., & Wallace, D. C. (1990) *Cell* 61, 931–937.
- Steinberg, S., & Cedergren, R. (1994) *Struct. Biol.* 1, 507–510.
- Steinberg, S., Gautheret, D., & Cedergren, R. (1994) *J. Mol. Biol.* 236, 982–989.
- Sussman, J. L., Holbrook, S. R., Warrant, R. W., Church, G. M., & Kim, S.-H. (1978) *J. Mol. Biol.* 123, 607–630.
- Ueda, T., Ohta, T., & Watanabe, K. (1985) *J. Biochem.* 98, 1275–1284.
- Ueda, T., Yotsumoto, Y., Ikeda, K., & Watanabe, K. (1992) *Nucleic Acids Res.* 20, 2217–2222.
- Wakita, K., Watanabe, Y., Yokogawa, T., Kumazawa, Y., Nakamura, S., Ueda, T., Watanabe, K., & Nishikawa, K. (1994) *Nucleic Acids Res.* 22, 347–353.
- Watanabe, Y., Kawai, G., Yokogawa, T., Hayashi, N., Kumazawa, Y., Ueda, T., Nishikawa, K., Hirao, I., Miura, K., & Watanabe, K. (1994) *Nucleic Acids Res.* 22, 5378–5384.
- Westhof, E., Dumas, P., & Moras, D. (1985) *J. Mol. Biol.* 184, 119–145.
- Wolstenholme, D. R. (1992) *Int. Rev. Cytol.* 141, 173–216.
- Woo, N. H., Roe, B. A., & Rich, A. (1980) *Nature* 286, 346–351.
- Yokogawa, T., Kumazawa, Y., Miura, K., & Watanabe, K. (1989) *Nucleic Acids Res.* 17, 2623–2638.
- Yokogawa, T., Watanabe, Y., Kumazawa, Y., Ueda, T., Hirao, I., Miura, K., & Watanabe, K. (1991) *Nucleic Acids Res.* 19, 6101–6105.
- Zacharias, M., & Hagerman, P. J. (1995a) *J. Mol. Biol.* 247, 486–500.
- Zacharias, M., & Hagerman, P. J. (1995b) *Proc. Natl. Acad. Sci. U.S.A.* 92, 6052–6056.

B1952329G